Proceedings of ASME Turbo Expo 2020
Turbomachinery Technical Conference and Exposition
GT2020
June 22-26, 2020, London, England

GT2020-15983

Quick Start of an Industrial Gas Turbine Engine through the Development of "Silent Start" VGV Schedule

Senthil Krishnababu, Vili Panov, Simon Jackson, Andrew Dawson

Siemens Industrial Turbomachinery Ltd, Lincoln, United Kingdom.

ABSTRACT

In this paper, research that was carried out to optimise an initial variable guide vane schedule of a high-pressure ratio, multistage axial compressor is reported. The research was carried out on an extensively instrumented scaled compressor rig. The compressor rig tests carried out employing the initial schedule identified regions in the low speed area of the compressor map that developed rotating stall. Rotating stall regions that caused undesirable non-synchronous vibration of rotor blades were identified. The variable guide vane schedule optimisation carried out balancing the aerodynamic, aero-mechanical and blade dynamic characteristics gave the 'Silent Start' variable guide vane schedule, that prevented the development of rotating stall in the start regime and removed the non-synchronous vibration. Aerodynamic performance and aero-mechanical characteristics of the compressor when operated with the initial schedule and the optimised 'Silent Start' schedule are compared. The compressor with the 'Silent Start' variable guide vane schedule when used on a twin shaft engine reduced the start time to minimum load by a factor of four and significantly improved the operability of the engine compared to when the initial schedule was used.

NOMENCLATURE

CFD	Computational Fluid Dynamics
Cp	Specific heat capacity (J/kg K)
EO	Engine Order
F	Frequency (Hz)
IGV	Inlet Guide Vane
ISBV	Inter-Stage Bleed Valve (Stage-6 bleed)
NSV	Non-Synchronous Vibration
S1,S2,S3	VGVs 1,2,3
T_o	Total temperature
U	Rotor speed at mid span (m/s)
V	Flow velocity at stage inlet
VGV	Variable Guide Vane
ρ	air density (kg/m^3)
ɵ	Probe separation angle (degrees)
Φ_s	Phase angle (degrees)
Φ	Flow Coefficient
Ψ	Loading Coefficient
ω	rotational speed (radians/s)

Subscripts

s	stall
r	rotor
1	Stage inlet
2	Stage exit

INTRODUCTION

Industrial gas turbines are typically used in power generation or mechanical drive applications. Multi-stage axial compressors with high efficiency and a wide operating range are commonly used in industrial gas turbines. The operability and stability of such multi-stage axial compressors are limited by phenomenon such as rotating stall and surge. The extent and the effect of these phenomena depend on the operating condition of the compressor. At lower speeds, typically, the front stages stall and the rear stages choke. This situation is reversed when operating near to design or full speed [1]. At lower speeds stall and surge are a consequence of larger flow incidence onto the front stages which are usually controlled by the use of either single to multiple bleed ports and/or variable stagger inlet guide vanes (IGV) along with single to multiple rows of variable guide vanes (VGV). When bleeds and variable vanes are used these are normally controlled against corrected speed. The stagger angle of the variable vanes, varied with speed, reduces the incidence to the following rotor blade which reduces the work done by the rotor blade. This results in reduction of incidence on to the following stator vane due to the increase in rotor exit axial velocity. However, this reduction in incidence might not be sufficient enough and hence the stagger angle of the downstream stator vane might also change with respect to speed [2]. Multi-stage axial compressor of an industrial gas turbine can typically have 4 or 5 such VGV rows. The variation in the stagger angles with respect to speed is usually called the VGV schedule.

Various studies have investigated and reported the effect of VGVs on compressor performance and operability. Mallett and Groesbeck [3] investigated the effect of inter-stage bleed valve and an IGV that can move between two predetermined positions on the knee in stall line and on the rotating stall characteristics of a 16-stage axial compressor. They found that the largest improvement in stall margin that eliminates the knee in stall line and a four-cell rotating stall in the low speed regime was due to the combined effect of keeping the bleed open and closing of the IGVs. i.e. increasing the stagger angle.

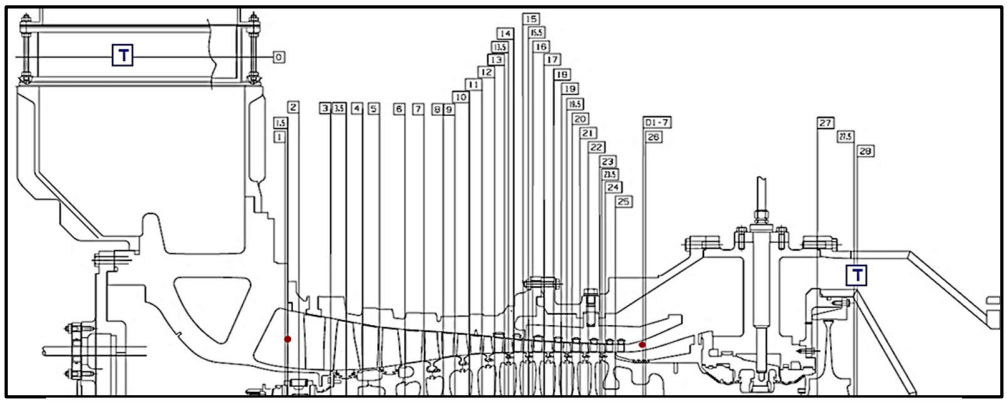

T Inlet (Plane-0) and Exit total temperature (Plane-28)

• Inlet (Plane-1.5) and Exit Total pressure rake (Plane-26)

Stator leading edge total pressure and total temperature probes (Planes 2,4,6…24 and 25)

Hub (Planes 1, 26, D1 to D7) and Casing (Planes 1 to 28, D1-D7) static pressure tapings.

Tip timing probes on Rotors 1,2,3,4,5 and 6.

KULITES in Planes 3, 13 and 19 (4 around the circumference)

FIGURE 1 CROSS SECTION OF THE TEST COMPRESSOR

Sun and Elder [4] reported an algorithm based on one-dimensional mean-line method for optimization of VGV angles in a seven-stage axial compressor. Although such conclusions were known at that time, they have demonstrated and quantified the benefits of varying the stagger of the front stages which provides a powerful technique to rematch the stages in order to obtain a high overall performance with a wider surge-free flow range. Gallar et al. [5] by integrating a genetic algorithm optimizer with a mean-line method demonstrated improvements in compressor performance while keeping an adequate surge margin by scheduling of the VGVs. Kim et al. [6] by performing a full engine analysis at design and off-design conditions have derived scheduling of VGVs for a three-stage compressor. It was reported that the performance of the engine due to scheduling of IGV and the two VSVs was better than that of the engine with IGV only scheduling because of improved efficiency of the axial part of high-pressure compressor in off-design condition. Reitenbach et al. [7] presented a multidisciplinary numerical method that combines the compressor through-flow analysis tool with engine performance tools, for the optimisation of the VGV scheduling. They have reported that surge margin can be improved with modified VGV settings while keeping the penalty on thrust specific fuel consumption within acceptable limits.

The optimisation of one such VGV schedule, albeit an initial schedule, for a multistage compressor using a compressor rig is presented in this paper. The use of the compressor with the optimised schedule in a twin shaft engine reduced the start-up time to minimum load by a factor of four and improved low speed operability compared to the initial schedule.

1 Test Vehicle

A cross section of the research compressor showing the instrumentation planes is presented in Fig. 1. In addition to the instrumentation for overall compressor performance measurements taken from inlet and exit total pressure and total temperature rakes; stator vane leading edge total pressure and total temperature probes, hub and casing static pressures probes, tip timing probes eight per stage on stages-1 to 6 and high frequency pressure transducers (Kulite; four per stage) at inlets to rotor-1, 6 and 9 were provisioned.

The research compressor is a high-speed compressor comprising of eleven stages with a variable stagger IGV row followed by three rows of VGVs and an inter-stage bleed port downstream of stage-6. Blade and vane profiles are of modern multi-circular arc 3D design. Rotor-1 inlet Mach number is transonic. Rotor blade tip and stator vane hub clearances vary from approximately 1% to 3% of blade height from the front to rear blade rows.

2 Initial VGV Schedule

The selection of appropriate IGV and VGV stagger angles at low speeds is crucial to achieve good off design compressor operating characteristics and hence trouble free starting once the compressor is integrated into the engine. In this research it is shown how a VGV schedule (a variant of a preliminary theoretical schedule) referred in this paper as ‘Initial Schedule’ used for the compressor rig was subsequently optimised and how this optimisation impacts the low speed operating characteristics of the compressor and the start-up characteristics of an engine. In the following sections the aerodynamic and aero-mechanical characteristics of the compressor operated with the ‘Initial Schedule’ is discussed.

2.1 Compressor Performance

Characterisation of the compressor began with several constant acceleration speed sweeps between 40% and 80%

corrected speed. These were carried out to record and analyse the tip timing data to ensure later running would not compromise the mechanical integrity of the compressor. Following these an overall performance map of the compressor was recorded. At a given speed for a given operating point the compressor performance data, particularly the polytropic efficiency was monitored with respect to time and a full data set was recorded once the performance parameters converged. The full data set includes the overall performance parameters, hub and casing static pressures, stator vane leading edge total pressures and temperatures. Five to seven performance points per speed were recorded (see Fig. 2) by adjusting the exit valve. In this figure mass flow and pressure ratio are normalised using the design point mass flow and pressure ratio respectively. The work reported here looks at the possibilities of improving the performance characteristics. Other information included in this figure is discussed in the following section.

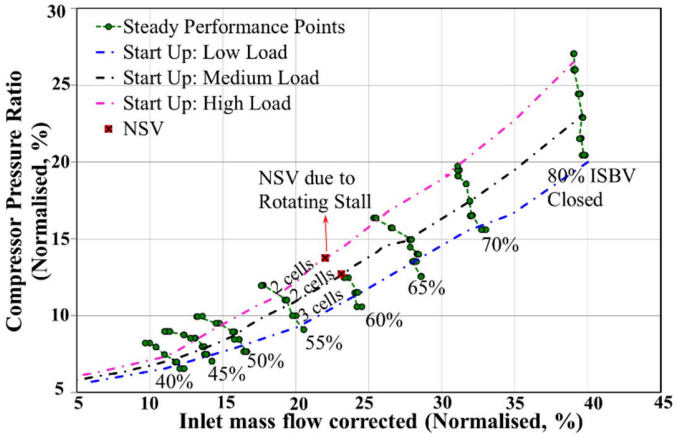

FIGURE 2 COMPRESSOR MAP FROM 40% TO 80% CORRECTED SPEEDS: INITIAL SCHEDULE

2.2 Rotating Stall and Blade Vibrations Characteristics

Following the steady state mapping, various start-ups, i.e. compressor accelerated to 80% corrected speeds with different exit valve settings, i.e. various compressor pressure ratios (represented by names low load, medium load and high load in Fig. 2) were carried out. During these start-ups tip timing measurements and high frequency pressure (Kulite) measurements were taken. Figure 3 shows the spectral data coloured by amplitude of pressure perturbation normalised by inlet total pressure of the signal recorded by one of the probes on rotor-6 plotted against the rotor speed along the high load line shown in Fig. 2. Figure 4 shows the coherence (cross-correlation), normalised amplitude and phase difference between the signals as seen by two probes that are apart by 79° in this case. Coherence i.e. cross-correlation of the signal between the probes of close to 1 implies a well-established disturbance. The stronger the cross-correlation, the larger is the chance of the disturbance reappearing. So, coherence of 1 would imply a well-established rotating stall. Utilising the frequency (normalised by first engine order at design speed) of a peak disturbance (at 'C' as marked in Fig. 4) and its phase difference with the probe 79° apart (see Table 1), the number of cells and its speed can be calculated using the following relationship as reported in [**8**].

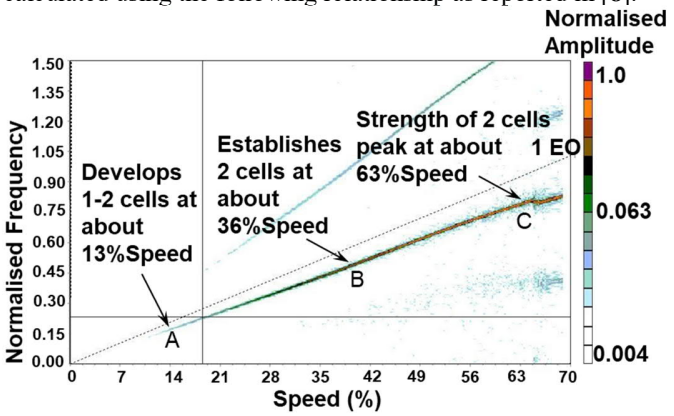

FIGURE 3 SPECTRAL ANALYSIS OF TRANSDUCER ON ROTOR-6 (ALONG HIGH LOAD LINE)

Table 1 MARKER 'C' (SEE FIG. 4) PARAMETERS

Marker	Normalised Frequency (F_s)	Phase (Φ_s)	Probe Separation Angle (θ)	Normalised Rotor Frequency (F_r)
C	0.81	162	79°	0.94

$$N = \text{Integer}(\Phi_s/\Theta) = 2 \quad (1)$$

$$\text{Speed of Stall Cells} = F_s / (F_r * \Phi_s/\Theta) = 42\% \quad (2)$$

F_r is the rotor frequency when 'C' occurs. Speed of stall cells so calculated were verified by calculating it alternatively using the time history of the static pressure. Figure 5 shows the time history of static pressures recorded by the four probes on rotor-6. It should be noted that values of probes PB, PC and PD are shifted by a constant value for purpose of clarity. Using the separation angle between probes PA and PD ($=\Theta_{AD}$) and the time lag of the peak (Del-T in seconds) as marked in Fig. 5 speed of the stall cells is calculated as follows.

$$\text{Speed of Stall Cells} = \omega_s / \omega_r = 42\%, \quad (3)$$

where ω_r is the angular speed of the compressor and ω_s ($=\Theta_{AD}$ /Del-T) is the angular speed of the stall cells. From similar analysis performed at markers 'A' and 'B' of Fig. 4 it was established that the rotating stall develops from about 13% speed when the coherence starts to build up to 1.0 and established into a two cell pattern at about 36% speed when the coherence is 1.0 as noted in Fig. 3. The strength of the stall cells peaks at about 63% speed as indicated by coherence of 1.0 and maximum amplitude of 0.2. Similar analysis of the Kulite data have shown that during start-up the compressor develops 3 cells if the load (i.e. pressure ratio) is low but develops 2 cells if the load is mid to high (as marked in Fig. 2).

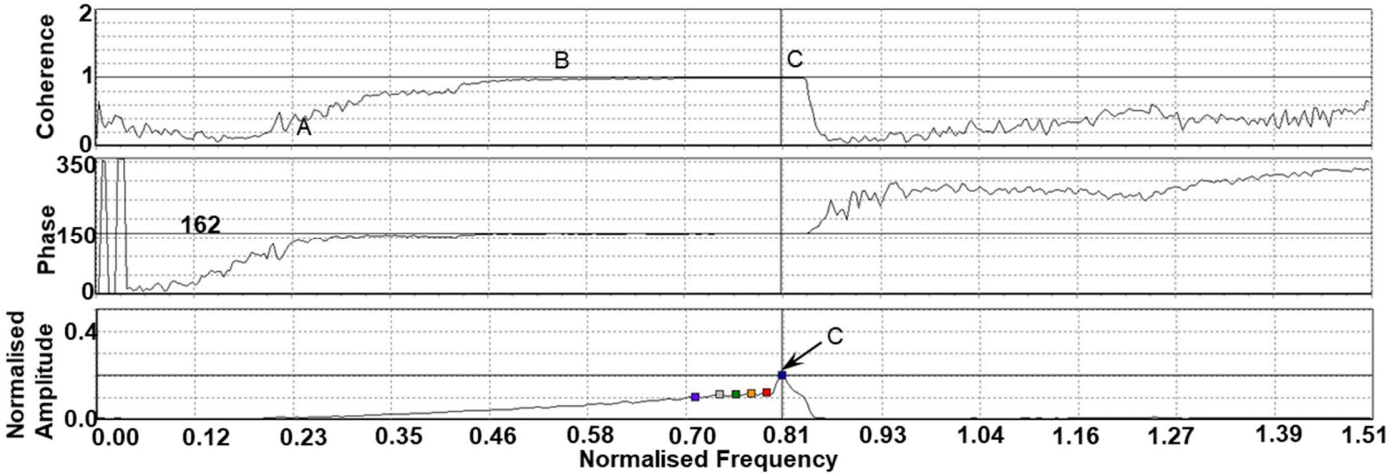

FIGURE 4 CROSS-CORRELATION OF PRESSURE SIGNAL BETWEEN TWO PROBES 79° APART ON STAGE-6

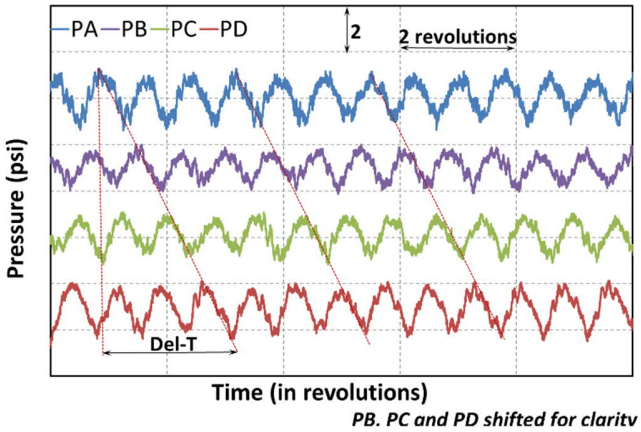

FIGURE 5 PRESSURE SIGNAL FROM PROBES ON STAGE-6

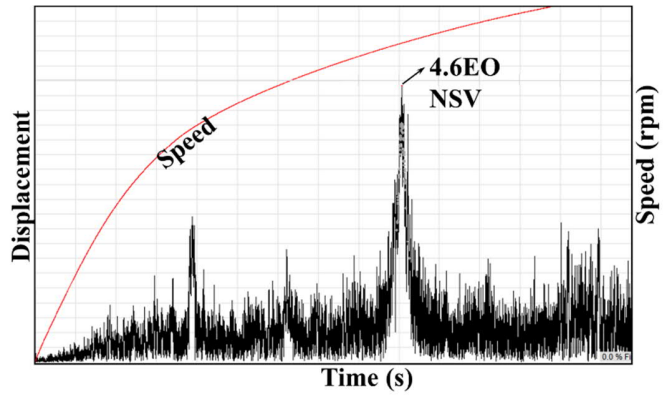

FIGURE 6 A ROTOR BLADE RESPONSE AT OPERATING POINT SHOWN IN FIGURE ON HIGH LOAD LINE

It is not unusual for rotating stall described above to cause non-synchronous vibration of rotor blades. Occurrence of two such non-synchronous vibration of a rotor blade caused by the rotating stall as measured by the tip timing probes described above during the medium load and high load start-up is superimposed on the compressor map shown in Fig. 2. Figure 6 shows a 4.6EO mode-1 response of one of the rotor blades at high load as an example. Although the amplitude of response was with-in allowable limits it is undesirable. Thus, the schedule was optimised for corrected speeds from 40% to 80% in order to improve aero-mechanical characteristics. Subsequent tests carried out to optimise the VGV schedule are described in the following sections.

3 Optimisation of VGV Schedule

Initially attempts to manually optimise the VGV settings at 70% corrected speed were made. 70% corrected speed was chosen as it was low enough for the rotating stall to still exist and high enough for CFD validation to be performed in the future. As noted in [**9**] in which such validation is carried out, speeds any lower than this are expected to be challenging for CFD from convergence point of view. In [**9**] ability of URANS in predicting rotating stall is demonstrated. Individual performance characteristics of the first four stages were used to aid in the optimisation process. Performance of stages-1 to 4 with 'Initial settings' represented by the flow coefficient and loading coefficient is shown in Fig. 7. These coefficients were calculated using the spanwise average value of measured stator vane leading edge total pressure, leading edge total temperature and static pressure measured at the casing using standard gas dynamic equations and using standard definition as the following.

$$\Phi = \frac{V}{U} \tag{4}$$

$$\Psi = \frac{C_p(T_{o2} - T_{o1})}{\rho U^2} \tag{5}$$

It should be noted that since parameters measured at vane leading edges are used to calculate performance, the phrase 'stage performance' implies that of a stage from upstream vane leading edge to downstream vane leading edge. In Fig. 7 direction of the pointer represents the direction of increase in overall compressor pressure ratio. It can be seen that stage-4 is stalled and that stage-3 represent an interesting trend (see Fig. 7b) in which the flow coefficient initially drops with increase in

overall compressor pressure ratio and then suddenly increases with a step change to only decrease again. This step increase in flow coefficient is due to the sudden change in number of stall cells from 3 to 2 as overall pressure ratio is increased as noted in Fig. 2. In summary stages 3 and 4 are stalled and that optimisation of VGV settings was carried out to improve the performance of these stages.

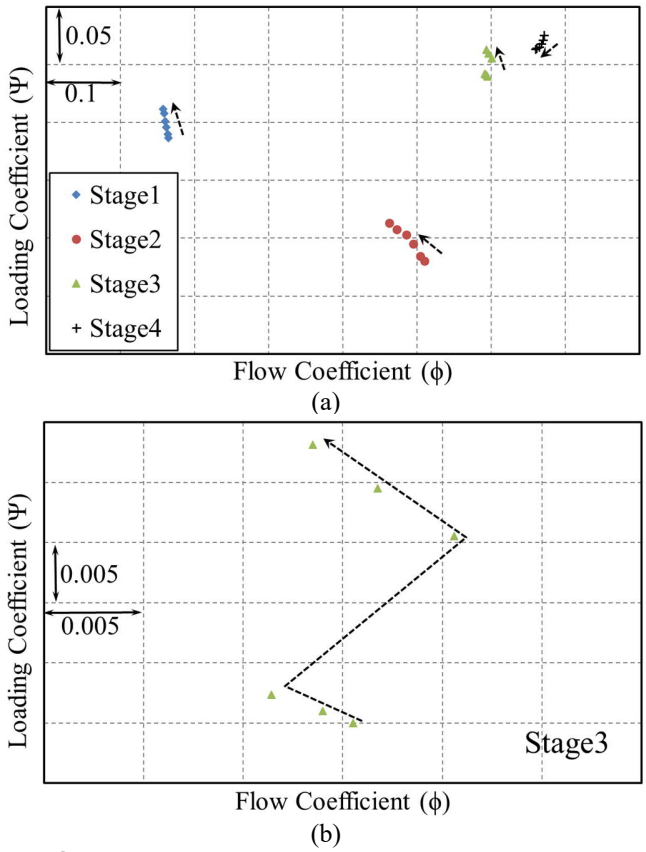

FIGURE 7 (A) PERFORMANCE CHARACTERISTICS OF STAGES 1 TO 4 (B) CLOSER VIEW OF STAGE-3 CHARACTERISTICS: 'INITIAL SCHEDULE'

Various VGV settings as shown in Table 2 were employed in an attempt to improve the performance of stages-3 and 4 without compromising the performance of other stages. For each of these cases in the table, VGVs were adjusted while keeping the compressor operating at 70% corrected speed and the speed line was recorded along with the full data set to calculate the stage performances. During this process, online analysis (i.e. live analysis) of Kulite data to assess the rotating stall (i.e. frequency, amplitude, etc.) and the tip timing measurement data to monitor the blade dynamics in order to keep the compressor in the safe operating limits were carried out. In case of the 'Initial schedule', IGV and the VGVs were closed with respect to a preliminary schedule by 6°, 1°, 1° and 3° respectively. The amount of closures was decided based on the experience with similar products. This 'Initial schedule' as shown in the previous sections isn't satisfactory from aero-mechanical performance point of view. Hence, the alternative option of opening the IGV going against the conventional wisdom of closing the IGVs and VGVs when stall is encountered was explored.

Table 2 VGV OPTIMISATION

Case name	IGV	S1	S2	S3
Initial Schedule*	6	1	1	3
Case-A**	-6	0	0	0
Case-B**	-6	-4	0	0
Case-C**	-6	0	-3	0
Case-D**	-6	3	-3	0
Case-E**	-6	3	-3	-3
Case-F**	-10	0	0	0
Case-G**	-10	0	5	0
Case-H**	-10	0	9	0

**Values as a change from preliminary schedule. **Change with respect to Initial Schedule (changes marked by grey cells).*

Initially, IGV was opened by 6 degrees putting it back to the position it was in case of the preliminary schedule maintaining other VGV stagger angles same as in 'Initial schedule' (Case A). The effect of doing so on-stage performance, rotating stall and blade dynamic characteristics were assessed by recording full data set for five to seven overall compressor performance points. Objective here was to redistribute the loading between these stages, thus, to ease the loading on the stalled stages. However, live analysis of data (Φ vs Ψ of the stages in particular) has shown that stage-1 was stalled too. This might be expected lines as the IGV was opened. Hence, S1 was opened (Case B). This drove stage-2 too to stall. Hence, S1 was closed back and S2 was opened (Case C) in an attempt to address stage-2 stall. However, as shown in Fig. 8 stage-3 too stalled, hence S1 was closed further (Case-D). Subsequently, various trails represented by Cases E to H were made. The use of Case-H VGV settings resulted in a significant reduction in the strength of rotating stall and corresponding improvement in stage performances. Hence these settings were employed at 40% corrected speed to record the speed line and the full data set. As these settings weren't optimum at 40% speed, following similar process as at 70% speed, the VGV settings at 40% speed were optimised to be "-13°, 5°, 11°, 9°" (change in comparison to the 'Initial Schedule'). VGV settings at 70% speed was then revisited and optimised further following similar process to be "-19°, -0.5°, -2.5°, 6°" (change in comparison to the 'Initial Schedule'). Performance of stages-1 to 4 with the new schedule named 'Silent Start' at 70% corrected speed is shown in Fig. 9. From this figure it is seen that none of the stages are stalled. The settings at other corrected speeds between 40% and 80% were then similarly adjusted. The VGV schedule so obtained is

compared to the 'Initial Schedule' in Fig. 10. Thus, as can be seen in figure at the closed end of the schedule (i.e. 40% speed and lower), IGV is opened by 13° whereas other VGVs are closed by 5°, 11° and 9° respectively compared to the initial schedule. These settings were gradually opened for higher speeds to result in IGV and Stator-1 open by 21° and 2° respectively and other two VGVs closed by 5° compared to the initial schedule. Hence, when compressor stall is encountered it may not be always essential to close all VGVs. This depends, as shown here, on the stages that are stalled and the blade rows that suffer adversely due to blade dynamic challenges caused by rotating stall.

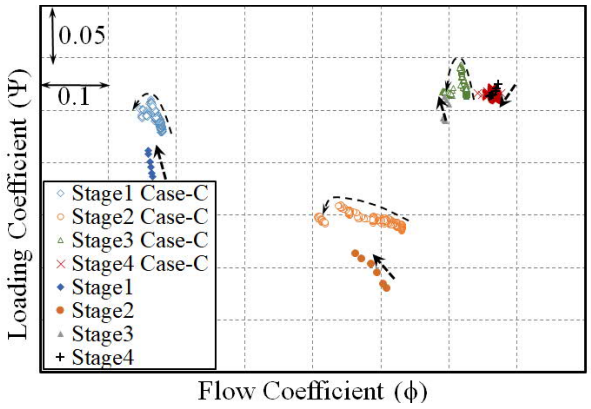

FIGURE 8 PERFORMANCE CHARACTERISTICS OF STAGES 1 TO 4: CASE-C VS 'INITIAL SCHEDULE'

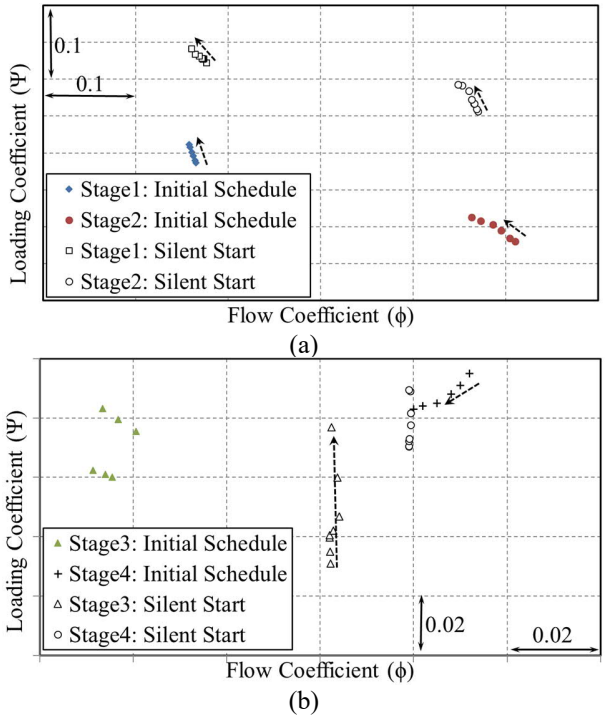

FIGURE 9 PERFORMANCE CHARACTERISTICS OF STAGES 1 TO 4: SILENT START SCHEDULE.

3.1 Silent Start Schedule: Compressor Performance

Figure 11 shows the performance of the compressor recorded using the 'Silent Start' VGV schedule along with the performance map recorded using the 'Initial schedule' for the purpose of comparison. There is indication of significant improvements to operating range (see the grey region marked in figure). It is also seen that compared to the 'Initial schedule' the compressor inlet mass flow has also increased. This is partly due to the IGV being more open compared to the standard settings and partly due to the absence of rotating stalls i.e. reduction in flow blockage.

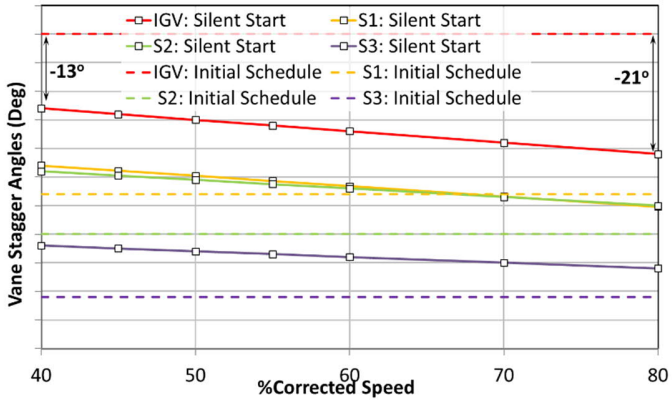

FIGURE 10 SILENT START VGV SCHEDULE

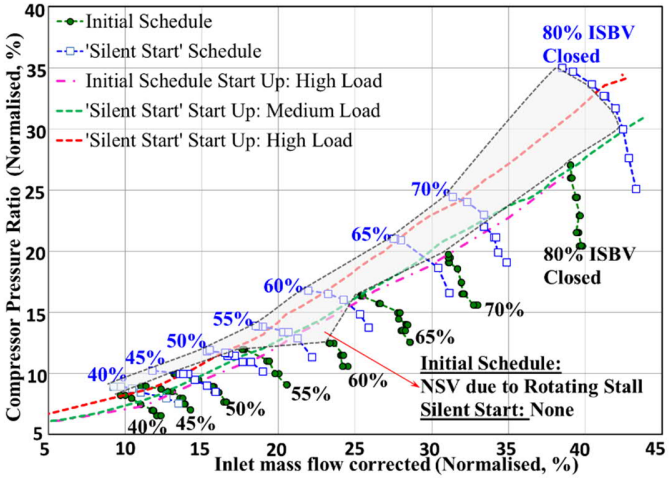

FIGURE 11 COMPRESSOR PERFORMANCE: INITIAL SCHEDULE VS SILENT START SCHEDULE

3.2 Silent Start Schedule: Rotating Stall and Blade Vibrations Characteristics

As with the standard schedule, various start-ups to 80% speed were carried out to record the high frequency pressure (Kulite) and tip timing data. As the indicated stability margin in case of the 'Silent Start' settings is higher than that due to 'Initial schedule', the new medium load line is very close to the high load in case of initial settings (see Fig. 11).

Figure 12 shows the spectral data of the pressure signal recorded by one of the probes on stage-6 plotted against the rotor speed for the medium load start up with 'Silent Start' schedule.

It can be seen that no rotating stall develops on this start up. Initial stall that develops at very low speed at about 8% speed dissipates at about 23% speed. For the low load and high load start up's too no rotating stall developed, thus avoiding any NSV events.

This demonstrates the possibility of optimisation of the VGV schedule by balancing the aerodynamic, aero-mechanical and blade dynamic characteristics thus achieving rotating stall free and NSV free operation of a modern transonic compressor with significant improvements to operating range.

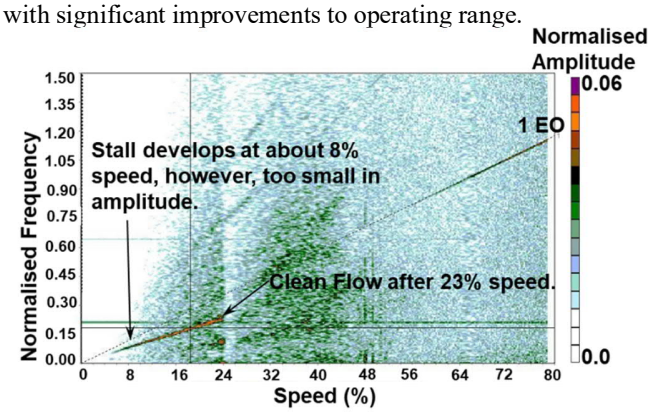

FIGURE 12 SPECTRAL ANALYSIS OF TRANSDUCER ON ROTOR-6 (START UP TO 80% SPEED WITH MEDIUM LOAD): SILENT START

4 Application of Silent Start VGV Schedule to a New Engine

The 'Silent Start' schedule developed was employed in the development of compressor for a new engine design. The 'Initial schedule' was also tested alongside for comparison purposes. Various acceleration rates, named accel-1 to accel-4 were used to start the engine to 80% corrected speed (see Fig. 13). In case of 'Initial schedule', in order to address lower indicated operating range at lower speeds acceleration rates were temporarily reduced in the region of concern (Accel-1). When 'Silent Start' schedule was employed acceleration rates were either reduced for a smaller speed range (Accel-2) or kept constant (Accel-3) or increased temporarily (Accel-4). Comparing the time to start (see Table 3) for these trial runs it can be seen that the engine start time is at least 4 times faster with the 'Silent Start' schedule.

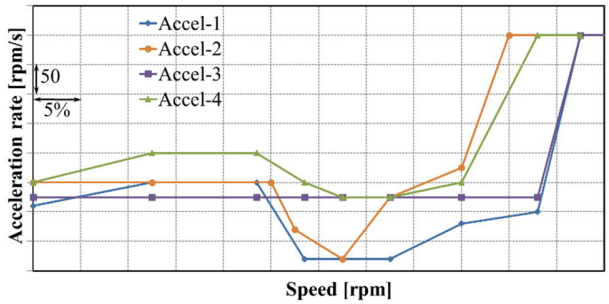

FIGURE 13 SPEED VS ACCELERATION: VARIOUS ENGINE STARTS EMPLOYING SILENT START AND INITIAL SCHEDULES

CONCLUSIONS

Research was carried out on a scaled multistage high-pressure compressor to optimise an initial VGV schedule. The compressor rig testing carried out showed the 'Initial schedule' had regions in the compressor map that develop rotating stall. Rotating stall regions that caused NSV of a rotor blade were identified. An interesting trend in stage performance in which the flow coefficient initially dropped as one would expect with increase in overall compressor pressure ratio but then suddenly increased with a step change to only decrease again due to the sudden change in number of stall cells from 3 to 2 as overall pressure ratio is increased was noticed.

Optimisation of the VGV schedule using a design of experiments approach resulted in the 'Silent Start' VGV schedule. This schedule prevented the development of rotating stall in the start regime, removed the NSV and significantly increased the compressors low speed operating range. During the optimisation, it was found that, when compressor stall is encountered it may not be always essential to close all VGVs.

The VGV schedule was later employed on a twin shaft engine that showed the optimised scheduled reduced the time to idle by a factor of four.

Table 3 SPEED UP IN ENGINE START TIMES

Case	Speed Up in Start Time*
Accel-2	2.2
Accel-3	2.6
Accel-4	4.0

*with respect to Accel-1

ACKNOWLEDGEMENTS

Authors would like to thank Siemens for allowing the publication of this research and Roger Wells for his support and comments. Help and support received from test and validation team is gratefully acknowledged.

REFERENCES

1. Day, I. J., 2016, "*Stall, Surge, and 75 Years of Research*", Journal of Turbomachinery, Vol. 138.
2. Gallimore, S.J., 1999, "*Axial Flow Compressor Design*", Proc Instn Mech Engrs, Vol 213, Part C, p 437.

3. Mallett, W. E., and Groesbeck, D.E., 1956, "*Effects of compressor interstage bleed and adjustable inlet guide vanes on compressor stall characteristics of a high-pressure-ratio turbojet engine at altitude*", NACA RM E55G27.
4. Sun, J., and Elder, R. L., 1998, "*Numerical optimization of a stator vane setting in multistage axial-flow compressors*", Proc. Inst. Mech. Eng. A, J. Power Energy 212 (1998) 247–259.
5. Gallar, L, Arias, M, Pachidis, V., and Pilidis, P, 2009, "*Compressor variable geometry schedule optimisation using genetic algorithms*", ASME-GT-60049.
6. Kim, S., Kim, D., Son, C., Kim, K., Kim, M., and Min, S., 2015, "*A full engine cycle analysis of a turbofan engine for optimum scheduling of variable guide vanes*", Aerospace Science and Technology, 47, 21-30.
7. Reitenbach, S., Schnos, M., Becker, R.-G., and Otten, T., 2015, "*Optimization of compressor variable geometry settings using multi-fidelity simulation*", ASME-GT-42832.
8. Levy, Y., Reissner, A., Pismenny, J., and Riess, W., 2002, "*Experimental study of rotating stalls in a four-stage axial compressor*", ASME-GT-30362.
9. Krishnababu, S.K., 2020, "*On the Prediction of Rotating Stall in an Industrial Gas Turbine Compressor*", ASME-GT-15330.

